Turbulent Transport Properties for Axisymmetric Heterogeneous Mixing

VICTOR ZAKKAY,* EGON KRAUSE,† AND STEPHEN D. L. WOO‡
Polytechnic Institute of Brooklyn, Freeport, N. Y.

An experimental investigation of the turbulent mixing of two dissimilar gases is presented. This investigation was carried out in the mixing region of two coaxial jets to determine the turbulent transport coefficients for hydrogen-, helium-, and argon-air mixtures. The different gases were injected from the inner jet at either subsonic or supersonic speeds into an air stream maintained at a constant Mach number $M_e = 1.6$. The basic differential equations describing the mean flow properties are solved for the transport coefficients. The convective derivatives that are needed in the solution of the equations are determined from the velocity and concentration profiles measured in the experiments. Values of the eddy viscosity, turbulent diffusion coefficient, and Lewis number were evaluated in this manner and the eddy viscosity so obtained is then compared with existing formulations. A new formulation for the eddy viscosity is then given whereby existing theories may still be used in analyzing the mixing process. Finally, the influence of the form of the velocity and concentration profiles on the transport properties is discussed. Similarity parameters developed for the flow region downstream from the potential core are shown to be valid in both axial and radial directions for various injected gases.

Nomenclature

A, B = constants defined in Eq. (21)
D_t = turbulent diffusion coefficient
D_{12} = laminar binary diffusion coefficient
h_i = static enthalpy of species i
H = stagnation enthalpy
k = parameter defined in Eq. (22)
k_t = turbulent thermal conductivity
Le_t = turbulent Lewis number $= \rho D_t \bar{c}_p / k_t$
m = parameter defined in Eq. (22)
M = Mach number
n = parameter describing the decay of the centerline of the jet
p = pressure
P = Y_2 or $1 - U/1 - U_j$
P_t = turbulent Prandtl number $= \mu_t \bar{c}_p / k_t$
P^* = $Y_2/Y_{\text{℄}}$ or $1 - U/1 - U_{\text{℄}}$
r = radial coordinate
r_0 = radius of the jet
$\bar{r}, \bar{x}$ = normalized coordinate with respect to the radius of the jet
Re_e = Reynolds number per inch of the outer jet
Sc_t = turbulent Schmidt number $= P_t/Le_t$
u, v = velocity components in x and r directions, respectively
$\bar{u}$ = normalized velocity component with respect to u_j
U = u/u_e
x = axial coordinate
x_0 = length of the potential core
$\bar{x}$ = x/x_0
Y_i = mass fraction of species i
Y_1 = mass fraction of O_2
Y_2 = mass fraction of injected gas
Y_3 = mass fraction of N_2
ϵ = eddy viscosity
$\varkappa$ = constant defined in Eq. (28)
λ = $\rho_j u_j / \rho_e u_e$
μ_t = turbulent viscosity $= \rho\epsilon$
ξ = transformed axial coordinate
ρ = density
$\bar{\rho}$ = normalized density with respect to ρ_j
ψ = stream function

Subscripts

℄ = centerline
j = jet
e = external stream
t = turbulent

Presented as Preprint 64-99 at the AIAA Aerospace Sciences Meeting, New York, January 20–22, 1964; revision received June 16, 1964. This research was sponsored by the Aerospace Research Laboratories, Office of Aerospace Research, U. S. Air Force, under Contract AF 33(616)-7661, Project 7064, and is partially supported by the Ballistic Systems Division. The work presented here was initiated by Antonio Ferri, and the authors take this opportunity to thank him for his discussions.

* Research Associate Professor, Aerospace Engineering. Member AIAA.
† Research Associate. Associate Member AIAA.
‡ Research Assistant. Deceased September 29, 1964.

1. Introduction

THE problem of the turbulent free mixing of two coaxial gas streams has received considerable attention during recent years. One of the main difficulties in the analysis of turbulent mixing processes stems from the lack of information about the dependence of the turbulent transport coefficients on the flow properties. Therefore, it is the purpose of this paper to determine experimentally some of these transport properties.

Forstall and Shapiro[1] have treated this problem for incompressible flow by using the analysis of Ref. 2. The authors concluded that, for the flow fields investigated, mass diffusion was more rapid than momentum diffusion. Furthermore, the turbulent Pr_t and Sc_t numbers were found to be almost constant throughout the whole mixing region, being approximately equal to 0.70.

Recently several new methods of analysis have been developed for treating the problem of turbulent jets. The principles of these methods are discussed in Ref. 3, and the details may be found in Refs. 4–10. Of particular interest for the present analysis are Refs. 4 and 5. There, an analytical solution was presented for Pr_t, Sc_t, and Le_t equal or close to unity, such that the momentum, species, and energy equations could be related to each other. Also, in Ref. 5, semiempirical equations were derived in order to determine the eddy viscosity, Sc_t and Pr_t numbers, along the centerline. Since this technique was established on the assumption that Sc_t and Pr_t numbers are close to unity, it has not been shown yet whether the solution can be extended to flows where Pr_t and Sc_t numbers differ markedly from one.

This was the case for H_2-air mixtures investigated in Ref. 11, where apparent Sc_t numbers were evaluated along the centerline using the method of Ref. 5 and were shown to be of the order of 2 and higher. It was also demonstrated in Ref. 11 that Sc_t numbers different from unity have only a negligible influence on the development of the radial profiles. However, as pointed out in Ref. 3, the value of the Sc number may remarkably influence the form of the centerline decay for laminar flows, and it is therefore believed that a similar behavior might be observed in turbulent flows.

In connection with the last point mentioned, it is noted that Prandtl's formulation for the eddy viscosity is not valid any more in flows where large density gradients occur, as in the supersonic mixing process of hydrogen and air. This was shown in Ref. 12. Based on various assumptions, several new formulations for the eddy viscosity have been given, among others, Refs. 3, 11, and 12. In some cases[11] the analytically determined decay compares with the experimental data; however, the validity of these formulations has not been shown in general.

Therefore, a different approach to the problem is taken in the present analysis. The momentum, conservation of species, and energy equations are solved for the turbulent viscosity μ_t, the turbulent diffusion coefficient D_t, and the turbulent Le_t number. The resulting equations are integral differential equations that can be solved when the mass concentration, velocity, density, and stagnation enthalpy profiles are known. A similar analysis was made in Ref. 18. Therein the turbulent mass diffusion coefficient D_t was determined along the centerline of a wake produced by a two-dimensional porous cylinder. Helium and argon were injected through the porous surface into the surrounding air stream.

Experiments were conducted at the Polytechnic Institute of Brooklyn Aerodynamic Laboratory (PIBAL) facility for the purpose of obtaining information in the mixing region of two dissimilar gases. The apparatus consisted of two coaxial jets, the center one being either subsonic or supersonic, while supersonic flow ($M_e = 1.6$) was maintained in the outer jet. In order to study the influence of various injected gases on the transport properties, hydrogen, helium, argon, and carbon dioxide§ were used in the central jet of the apparatus. Measurements of mass concentrations and velocity were taken in the mixing region of the two gases for various initial conditions. Finally, similarity parameters are derived systematically from Ref. 5.

2. Theoretical Analysis

General Equations

The governing equations for the coaxial turbulent mixing of two dissimilar gases have been given in Refs. 4, 5, 12, and 13. In these, it is assumed that the mean turbulent flow quantities are described by the equations for laminar flow if the transport coefficients replace their molecular counterparts:

Conservation of Mass

$$\frac{\partial}{\partial x}(\rho u) + \frac{1}{r}\frac{\partial}{\partial r}(\rho v r) = 0 \tag{1}$$

Conservation of Momentum

$$\rho u\frac{\partial u}{\partial x} + \rho v\frac{\partial u}{\partial r} = \frac{1}{r}\frac{\partial}{\partial r}\left(\rho\epsilon r\frac{\partial u}{\partial r}\right) \tag{2}$$

Conservation of Energy

$$\rho u\frac{\partial H}{\partial x} + \rho v\frac{\partial H}{\partial r} = \frac{1}{r}\frac{\partial}{\partial r}\left[\frac{\rho\epsilon}{P_t} r\frac{\partial H}{\partial r} + \frac{(P_t - 1)}{P_t}\rho\epsilon r u\frac{\partial u}{\partial r} + \frac{(Le_t - 1)}{P_t}\rho\epsilon r\sum_{i=1}^{N} h_i\frac{\partial Y_i}{\partial r}\right] \qquad i = 1, 2 \ldots N \tag{3}$$

§ The CO_2 measurements were taken from Ref. 11.

Conservation of Species

$$\rho u\frac{\partial Y_i}{\partial x} + \rho v\frac{\partial Y_i}{\partial r} = \frac{1}{r}\frac{\partial}{\partial r}\left(\frac{\rho\epsilon}{Sc_t} r\frac{\partial Y_i}{\partial r}\right) + \dot{w}_i \tag{4}$$

Since, in the present analysis, only flows without chemical reaction are considered, the rate of formation of species i is equal to zero, i.e., $\dot{w}_i = 0$.

It was shown in Ref. 13 that large pressure variations may occur in supersonic jet flows close to the jet. Therefore, the preceding equations would not give a true description of the variation of the flow properties in the immediate region of the jet, and the present analysis will be restricted to the region further downstream where the static pressure distribution is uniform, within experimental accuracy.

Solutions to the preceding equations may be obtained provided some assumptions are made concerning the transport coefficients. In this analysis, the reverse approach will be taken: the conservation equations will be used as defining equations for the transport properties. The flow quantities and their derivatives appearing in these equations will be obtained by experiments. The turbulent transport properties to be determined are the turbulent viscosity μ_t, the turbulent diffusion coefficient D_t of the mixture, and the turbulent Pr_t, Le_t, and Sc_t numbers. They are related to each other[14–16]:

$$P_t = Le_t Sc_t \tag{5}$$

After integration of Eqs. (1, 2, and 4) with respect to r, the following integral differential equations are obtained:

For the turbulent viscosity $\mu_t = \rho\epsilon$,

$$\rho\epsilon = \left[\int_0^r \frac{\partial}{\partial x}(\rho u^2) r'dr' + \rho v u r\right]\left[r\frac{\partial u}{\partial r}\right]^{-1} \tag{6}$$

For the turbulent diffusion coefficient D_t,

$$\rho D_t = \left[\int_0^r \frac{\partial}{\partial x}(\rho u Y_2) r'dr' + \rho v Y_2 r\right]\left[r\frac{\partial Y_2}{\partial r}\right]^{-1} \tag{7}$$

where Y_2 is the mass fraction of the injected gas. Equations (6) and (7) are identical if the mass fraction of the injected gas Y_2 is replaced by u, and D_t is exchanged with ϵ.

The turbulent Lewis number can be expressed through the energy equation as

$$Le_t = \frac{D_t\sum_{i=1}^{i=3}\left(\frac{\partial h_i}{\partial r} - h_i\frac{\partial Y_i}{\partial r}\right)}{\frac{1}{\rho r}\left[\int_0^r \frac{\partial}{\partial x}(\rho u H) r'dr'\right] + vH - D_t\sum_{i=1}^{i=3} h_i\frac{\partial Y_i}{\partial r} - \epsilon u\frac{\partial u}{\partial r}} \tag{8}$$

Furthermore, the turbulent Schmidt number, by definition, is equal to the ratio of the eddy viscosity ϵ and the diffusion coefficient D_t:

$$Sc_t = \frac{\left[\int_0^r \frac{\partial}{\partial x}(\rho u^2) r'dr' + \rho v u r\right]\frac{\partial Y_2}{\partial r}}{\left[\int_0^r \frac{\partial}{\partial x}(\rho u Y_2) r'dr' + \rho v Y_2 r\right]\frac{\partial u}{\partial r}} \tag{9}$$

and the expression for the turbulent Prandtl number follows from Eqs. (5) and (9).

The values of the transport coefficients along the centerline are obtained by substituting the integrated conservation of mass equation [Eq. (1)]:

$$v = -\frac{1}{\rho r}\int_0^r \frac{\partial}{\partial x}(\rho u) r'dr'$$

for v, and evaluating the limit of Eqs. (6–8) for r approaching zero. There result

$$\lim_{r\to 0}\rho\epsilon = (\rho\epsilon)_{\ell} = \left(\frac{\rho u(\partial u/\partial x)}{2(\partial^2 u/\partial r^2)}\right)_{\ell} \tag{10}$$

$$\lim_{r\to 0} \rho D_t = (\rho D_t)_{\text{℄}} = \left(\frac{\rho u(\partial Y_2/\partial x)}{2(\partial^2 Y_2/\partial r^2)}\right)_{\text{℄}} \tag{11}$$

$$\lim_{r\to 0} Sc_t = (Sc_t)_{\text{℄}} = \left(\frac{(\partial u/\partial x)(\partial^2 Y_2/\partial r^2)}{(\partial Y_2/\partial x)(\partial^2 u/\partial r^2)}\right)_{\text{℄}} \tag{12}$$

$$\lim_{r\to 0} Le_t = (Le_t)_{\text{℄}} = \left(\frac{D_t \sum_{i=1}^{i=3}\left(\frac{\partial^2 h_i}{\partial r^2} - h_i \frac{\partial^2 Y_i}{\partial r^2}\right)}{\sum_{i=1}^{i=3}\left(\frac{1}{2} u \frac{\partial h_i}{\partial x} - D_t h_i \frac{\partial^2 Y_i}{\partial r^2}\right)}\right)_{\text{℄}} \tag{13}$$

The solution of Eqs. (6–13) requires measurements of the following four flow properties throughout the flow field: 1) the mass concentration of the injected gas Y_2; 2) the static pressure distribution; 3) the stagnation pressure distribution; and 4) the stagnation temperature.

3. Correlation Parameters for Similar Profiles

It is necessary to determine all flow properties and their derivatives appearing in Eqs. (6–13) from the four measurements indicated previously. A considerable simplification in the correlation of the experimental data and a more accurate determination of the derivatives can be achieved if the flow in the mixing region exhibits similarity behavior, i.e., all measured profiles can be correlated into one single profile in terms of a suitable parameter. Therefore, it is desirable to investigate the governing parameters in the mixing region first. For this purpose, the asymptotic solution for the compressible turbulent jet with Pr_t and Le_t equal to unity[4, 5] will be discussed. The solution was established by applying the von Mises transformation to the conservation equations (1–4) and linearizing the equations in the transformed plane. The solution to the linearized equations is then given in terms of the so-called offset circular probability function P as tabulated in Ref. 17. Following the notation of Ref. 5, let P denote either Y_2 or $(1 - u/u_e)/(1 - u_j/u_e)$. The centerline decay in the transformed plane is given by

$$P_{\text{℄}} = 1 - \exp[-\psi_j^2/4\xi] \tag{14}$$

where ψ_j is the stream function of the inner jet, and is equal to $2^{1/2}$. The transformation equations are

$$\bar{r}^2 = \int_0^{\psi} \frac{\psi'}{\bar{\rho}\bar{u}}\, d\psi' \qquad \bar{x} = A \int_0^{\xi} \frac{d\xi}{2\rho\epsilon} \tag{15}$$

where A is a constant. If $\xi \to \infty$, the normalized P function $P^* = P/P_{\text{℄}}$ approaches the Gaussian distribution[17]

$$P^* = \exp[-\psi^2/4\xi] \tag{16}$$

since for $\xi \to \infty$, $\rho \to \rho_e$ and $u \to u_e$, the first of Eqs. (15) reduces to $\psi^2 = 2\bar{r}^2/\lambda$, where λ is the mass flux ratio of the inner to the outer jet. Hence, Eq. (16) becomes

$$P^* = \exp[-\bar{r}^2/2\lambda\xi] \tag{17}$$

Assuming that the centerline decay in the physical plane can be expressed by a law of the form $P_{\text{℄}} = \bar{x}^{-n}$, Eq. (17) reduces by means of Eq. (14) to

$$P^* = (1 - \bar{x}^{-n})^{\bar{r}^2/\lambda} \tag{18}$$

Thus, the asymptotic correlation parameter for the normalized profiles P^* is the expression $(1 - \bar{x}^{-n})^{\bar{r}^2/\lambda}$, since P^* remains constant as long as the right-hand side of Eq. (18) is constant for any combination of $\bar{x}$, $\bar{r}$, and λ.

It is also interesting to investigate the asymptotic spread of the jet. Consider now P^* and $\bar{x}$ as the independent variables and $\bar{r}$ as the dependent variable. If Eq. (18) is solved for $\bar{r}$ and differentiated with respect to $\bar{x}$, there is obtained

$$\frac{\partial \bar{r}}{\partial \bar{x}} = (-\lambda \ln P^*)^{1/2} \cdot \frac{n}{2} \frac{[-\ln(1 - \bar{x}^{-n})]^{-3/2}}{\bar{x}(\bar{x}^n - 1)} \tag{19}$$

which gives for $\bar{x} \to \infty$

$$\lim_{x\to\infty} \frac{\partial \bar{r}}{\partial \bar{x}} = (-\lambda \ln P^*)^{1/2} \bar{x}^{n/2-1} \tag{20}$$

For the case when the power n, describing the centerline decay, is equal to 2, $\partial\bar{r}/\partial\bar{x}$ for large values of $\bar{x}$ is equal to $(-\lambda \ln P^*)^{1/2}$, and $\bar{r}$ is then directly proportional to $\bar{x}$. This result is in agreement with the analysis of Ref. 3. Equations (19) and (20) also indicate that $\partial\bar{r}/\partial\bar{x}$ is proportional to the square root of the mass flux ratio λ. Thus, the spreading angle of the jet increases when the mass flux of the inner jet is increased with respect to the outer one.

Equations (16–20) are valid for large values of $\bar{x}$ only, and the experimentally determined profiles P^* in the mixing region may therefore be approximated by an exponential series of the form

$$P^* = \exp[-A\bar{r}^2 - B\bar{r}^4 \ldots] \tag{21}$$

In order to correlate the measurements directly without using the integral relations for the transformed coordinates, Eq. (21) is written in terms of the physical coordinate $\bar{r}$. It is therefore desirable to introduce ψ and ξ as given by Eq. (15) in a simplified form such as

$$\psi \sim \bar{r}/\lambda^k \qquad \xi \sim \bar{x}^m \tag{22}$$

It follows from Eq. (16) that Eq. (21) can be written as

$$P^* = \exp\left[-\frac{a\bar{r}^2}{\lambda^{2k}\bar{x}^{2m}} - \frac{b\bar{r}^4}{\lambda^{4k}\bar{x}^{4m}} \ldots\right] \tag{23}$$

where a, b . . . , and k and m are constants for each gas considered. Thus, if only the two terms $\bar{r}^2$ and $\bar{r}^4$ are retained, Eq. (23) can be solved for $\bar{r}$:

$$\ln\bar{r} = \tfrac{1}{2}\ln\{-\tfrac{1}{2}(a/b) + [\tfrac{1}{4}(a^2/b^2) - 1/b \ln P^*]^{1/2}\} + k \ln\lambda + m \ln\bar{x} \tag{24}$$

and, with a similar change of variables as in Eq. (19), there is obtained for constant values of P^*

$$\frac{\partial \ln\bar{r}}{\partial \ln\bar{x}} = \frac{\bar{x}}{\bar{r}}\frac{\partial\bar{r}}{\partial\bar{x}} = m$$
$$\frac{\partial \ln\bar{r}}{\partial \ln\lambda} = \frac{\lambda}{\bar{r}}\frac{\partial\bar{r}}{\partial\lambda} = k \tag{25}$$

The powers m and k, describing the spread of the jet as a function of $\bar{x}$ and the initial conditions λ, can be determined from the experiments without knowing the coefficients a and b. Lines of constant P^* are plotted as $\ln\bar{r} = f(\ln\bar{x})$, the inclination of which is then identical with m. Provided the profiles are similar, k may be evaluated in a similar manner.

When a, k, and m are known, the solution of the equations determining the transport coefficients along the centerline can be obtained readily. With the assumption that $P_{\text{℄}} = \tilde{x}^{-n}$, the profiles can be described as

$$P = \tilde{x}^{-n} \exp\left[-\frac{a\bar{r}^2}{\lambda^{2k}\tilde{x}^{2m}} - \frac{b\bar{r}^4}{\lambda^{4k}\tilde{x}^{4m}} - \ldots\right] \tag{26}$$

where $\tilde{x}$ is normalized by the initial length x_0, the length of potential core.

The solution of Eqs. (10) and (11) for ϵ and D_t may now be obtained using the assumed profile given in Eq. (26):

$$\left.\begin{matrix}\epsilon \\ D_t\end{matrix}\right\} = \frac{n\lambda^{2k} r_0^2}{4ax_0} u_e \cdot U_{\text{℄}} (P_{\text{℄}})^{(1-2m)/n} \tag{27}$$

The constants a, k, m, and n may have different values depending on whether momentum diffusion or mass diffusion is considered. For convenience let

$$\varkappa = n\lambda^{2k} r_0^2 u_e/4ax_0 \tag{28}$$

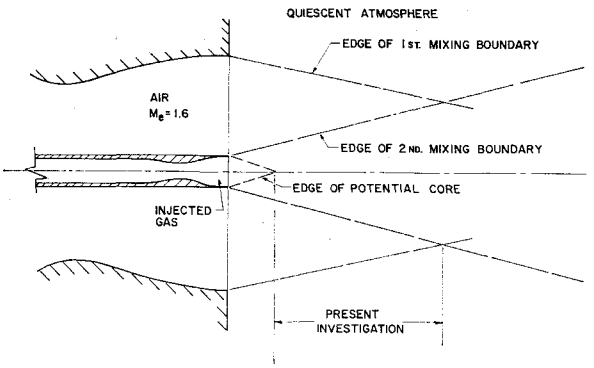

Fig. 1 Schematic of apparatus.

and $\varkappa_u$ may describe its value corresponding to the momentum diffusion and $\varkappa_{Y_2}$ its value for the mass diffusion; similarly, let m_u and m_{Y_2}, and n_u and n_{Y_2} describe the spread and decay of the velocity and concentration profiles. Then, Eqs. (27) can be written as

$$\epsilon = \varkappa_u U_{\text{℄}} \left(\frac{1 - U_{\text{℄}}}{1 - U_j}\right)^{(1-2m_u)/n_u}$$
$$D_t = \varkappa_{Y_2} U_{\text{℄}} (Y_{2\text{℄}})^{(1-2m_{Y_2})/n_{Y_2}} \tag{29}$$

For the case that m_u or $m_{Y_2} = \frac{1}{2}$, the dependence of ϵ and D_t on $[(1 - U_{\text{℄}})/(1 - U_j)]$ and $Y_{2\text{℄}}$ vanishes, and both the eddy viscosity and the diffusion coefficients are described by the constant $\varkappa$ times the centerline velocity.

It is also possible to express the eddy viscosity ϵ and the turbulent diffusion coefficient D_t in terms of the half boundary $\bar{r}_{1/2}$. By definition, $\bar{r}_{1/2}$ is evaluated where P^* in Eq. (23) is equal to 0.5. If only one term in Eq. (23) is retained, it follows from Eq. (24) that

$$\bar{r}_{1/2} = \left(-\frac{\ln 0.5}{a}\right)^{1/2} \lambda^k \bar{x}^m \tag{30}$$

Then, ϵ becomes, through Eqs. (10, 26, and 30),

$$\epsilon = (nr_0^2 u_e/4x_0)\lambda^{k/m}(-\ln 0.5)^{(1-2m)/2m} a^{1/2m} \bar{r}_{1/2}^{(2m-1)/m} U_{\text{℄}} \tag{31}$$

If Eq. (30) is compared with the integrated form of Eq. (20), it is seen that asymptotically $k = \frac{1}{2}$, $a = 1$, $m = n/2$, and $n = 2$. Further, as the experimental results will show, x_0/r_0 can be expressed by an equation of the form

$$\bar{x}_0 = K_1(\lambda)^{1/2} \tag{32}$$

and ϵ as given by Eq. (31) reduces to

$$\epsilon = K_2 u_e r_0 \bar{r}_{1/2} U_{\text{℄}} \tag{33}$$

where

$$K_2 = [2(-\ln 0.5)^{1/2} \cdot K_1]^{-1} \tag{34}$$

Equation (33) gives the asymptotic value of the eddy viscosity. It clearly shows that ϵ is proportional to the product of the half radius and the centerline velocity and has the same form as Prandtl's formulation in the problem of a jet exhausting into a quiescent atmosphere. Thus it is shown that this law holds true in the mixing process of two coaxial jets with different velocities. For the case of two jets having the same initial velocity, no momentum diffusion can take place, and ϵ is zero. This result is implied in Eq. (31) since the factor n, describing the decay along the centerline, is equal to zero.

It also follows from Eq. (31) that ϵ must not necessarily be a linear function of $\bar{r}_{1/2}$. For example, if m is equal to 0.5, the dependence on $\bar{r}_{1/2}$ vanishes, and ϵ is only proportional to the centerline velocity.

An expression for the turbulent diffusion coefficient in terms of the half radius and the centerline velocity may be obtained in like manner. For this case, the constant K_2 [Eq. (34)] has a different value, and the asymptotic value of the turbulent diffusion coefficient may be written as

$$D_t = K_3 u_e r_0 \bar{r}_{1/2} U_{\text{℄}} \tag{35}$$

The turbulent Schmidt number may be calculated either from Eqs. (29) or from Eqs. (33) and (35), which reduce to

$$Sc_t = \varkappa_u/\varkappa_{Y_2} \quad \text{or} \quad Sc_t = K_2/K_3 \tag{36}$$

for identical concentration and velocity profiles.

This is the result obtained in Ref. 1 for incompressible flows where it was pointed out that, for identical concentration and velocity profiles, the turbulent Schmidt number is independent of the external velocity and given by the ratio of two constants. The Lewis and Prandtl numbers can then be determined from Eqs. (13) and (5) using the derivatives for the velocity and concentration profiles evaluated from Eqs. (26). However, it is more advantageous to insert the numerical values of the derivatives in Eq. (13), since the complexity of the equation does not permit one to obtain a convenient form for the solution.

It cannot be expected that Eqs. (6) and (7) can be put into such simple forms as Eqs. (10) and (11). The main difficulty arises from the terms $\partial\rho/\partial x$ and ρ appearing on the right-hand side of Eqs. (6) and (7). Therefore, only numerical results of Eq. (6) will be given in Sec. 5.

4. Experimental Apparatus and Test Conditions

The experiments presented here were conducted in the hypersonic facility of the Polytechnic Institute of Brooklyn. The apparatus consisted of two coaxial jets, the center one being either subsonic or supersonic. Two different nozzles with discharge diameter of 0.3 and 0.6 in. were used for the inner jet in order to detect whether the flow in the mixing region was affected by the development of the boundary layer on the walls of the inner jet. The outer jet had a test section diameter of 3.44 in. and was maintained at supersonic speeds.

The arrangement of the test apparatus is shown in Fig. 1. Both jets exhausted into a 12-in.-diam tube such that the mixing process took place in an open jet region, and the influence of the walls was eliminated.

The measurements were taken in a region between the end of the potential core and the point where the edges of the first and the second mixing boundary intersected; therefore, the disturbances originated by the edge of the first mixing boundary did not affect the measurements. The concentration of the injected gas was measured by means of a thermal conductivity cell. This method was successfully used in Refs. 11, 13, and 18, and furnished accurate measurements since the ratio of the thermal conductivity of the various injected gases to that of air was sufficiently large. The cell was accurately calibrated with known samples of gas mixtures, and the output of the bridge was read in millivolts. A calibration chart was constructed in order to convert the millivolt output of the cell into concentration for each of the gases. The samples were extracted by means of a sharp conical orifice, 0.012 in. in diameter, and expanded immediately into a 0.065-in. tube. This in turn was led to a solenoid valve and then into a sample bottle. Prior to testing, the whole system was evacuated into the micron range. During the test, the solenoid valve was opened when steady flow conditions prevailed, and closed after a few seconds. The sample was then analyzed after the test.

The mass flow of the injected gas was measured by a venturi located upstream from the inner jet. Test durations of the order of one minute provided adequate time for taking

Table 1 Test conditions for the hydrogen, helium, and argon experiments

Test series	T_{se}, °R	T_{sj}, °R	P_{se}, psi	M_e	D_j, in.	D_e, in.
(Ref. 13)	1350	520	50	1.55	0.60	3.44
I	1500	600	50	1.60	0.30	3.44
II	520	520	46	1.60	0.30	3.44

Jet gas	Test series	λ	u_j/u_e	M_j
H_2	(Ref. 13)	0.022	0.20	0.110
		0.052	0.42	0.235
		0.094	0.76	0.425
		0.140	1.14	0.645
H_2	I	0.107	0.768	0.430
	II	0.047	1.455	0.510
		0.072	1.690	0.600
		0.124	2.42	0.890
He	I	0.154	0.456	0.330
		0.288	1.10	0.870
He	II	0.103	1.10	0.510
		0.185	1.673	0.819
A	I	0.497	0.181	0.420
		1.07	0.310	0.770
		1.86	0.433	1.17
		2.97	0.515	1.605
A	II	0.590	0.531	0.822
		0.790	0.564	0.886
		0.976	0.617	0.996

pictures, samples, and measurements of pressure and stagnation temperature.

The static pressure for all tests was maintained at 13 psia. The Reynolds number per inch of the outer jet was varied from 7.3×10^4 to 1.2×10^6 by changing the stagnation temperature. The Mach number of the outer jet was maintained approximately at 1.6. Hydrogen, helium, and argon were used as the injected gas in the present series. All test conditions are given in Table 1.

5. Discussion of Experimental and Theoretical Results

In this section, the experimental results of the various test series will be discussed first. Thereafter, similarity parameters and equations developed in Secs. 2 and 3 will be applied to them in order to evaluate the transport properties.

It was pointed out in Ref. 13 for the first time that the centerline decay of the mass concentration for hydrogen is proportional to $\tilde{x}^{-2}$. Subsequently, additional experimental information has been obtained for argon, hydrogen, helium, and carbon dioxide. Some of these data were already included in Refs. 3 and 11. In Refs. 3 and 13, the centerline decay of the mass concentration was plotted in parametric form for different mass flux ratios vs $\tilde{x}$. All these measurements can be correlated into a single curve if the mass concentration is plotted vs $\tilde{x}$, where $\tilde{x}$ is defined as the ratio of the distance from the jet discharge to the initial length, i.e., the length of the potential core.

Figure 2 presents the experimental centerline decay of the mass concentration so correlated for the four injected gases H_2, CO_2, A, and He. The data presented comprise the results for 25 different test conditions and are compared to a decay corresponding to $\tilde{x}^{-2}$. It is clearly seen that the measurements agree well with this law, and the following is therefore concluded:

1) The form of the centerline decay is not affected by the molecular weight of the injected gas.

2) The centerline decay for the test conditions investigated here and for Refs. 11 and 13 is not the same as for low-speed flows. In Ref. 1 it was shown that for low-speed flows the mass concentration decays proportionally to $\tilde{x}^{-1}$.

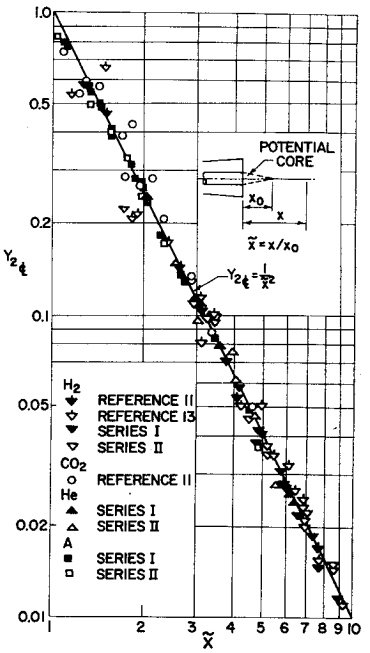

Fig. 2 Mass concentration of the injected gas at the centerline in the mixing region of the jet.

It was stated in Ref. 13 that the boundary layer on the inner jet may influence the mixing process. However, since the form of the decay remained the same for the whole range of Reynolds numbers investigated and for all nozzle configurations, the following can be concluded:

3) The form of the centerline decay is not affected by the boundary layer on the inner jet.

It now remains to define and explain the length of the potential core x_0. In this case, x_0 will be defined as the axial distance from the jet discharge to where the mass concentration of the injected gas is 99%, and may then be easily determined by plotting the centerline concentration on logarithmic paper. Since a distinct centerline decay was observed experimentally downstream from the potential core, the value of x_0 was determined by extending the line representing the centerline variation to the line of 100% concentration.

In Fig. 3, the initial length so obtained is plotted in the form $x_0/r_0 = \bar{x}_0$ vs the mass flux ratio λ. The dependence of $\bar{x}_0$ on λ was previously suggested in Ref. 13, and it is seen that a good correlation is obtained for the present data. In a first approximation, this dependence could be represented by an equation of the form $\bar{x}_0 \cong 22(\lambda)^{1/2}$. Although the form of the centerline decay was not affected by the development of the boundary layer on the inner jet, such influence is noticed for the variation of the initial length $\bar{x}_0$ with λ.

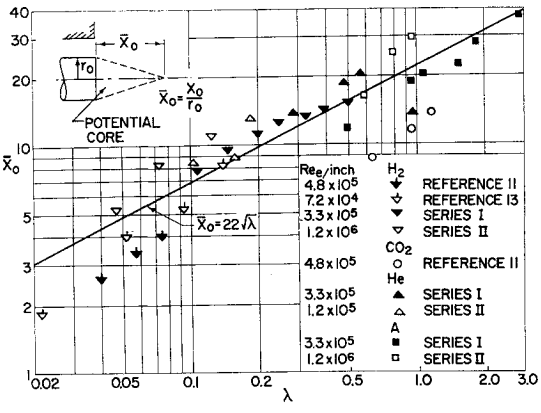

Fig. 3 Length of the potential core for the mass concentration decay as a function of the mass flux ratio $\lambda = \rho_j u_j / \rho_e u_e$.

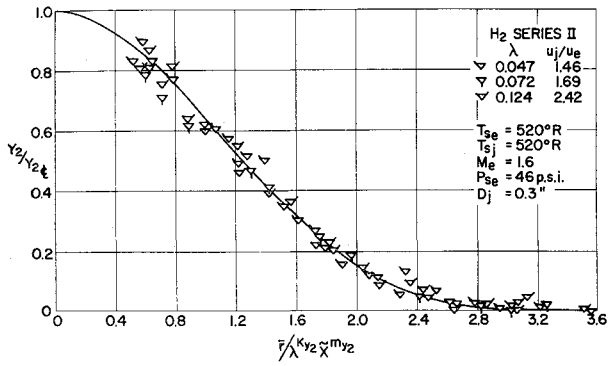

Fig. 4 Correlated radial mass concentration profiles for hydrogen.

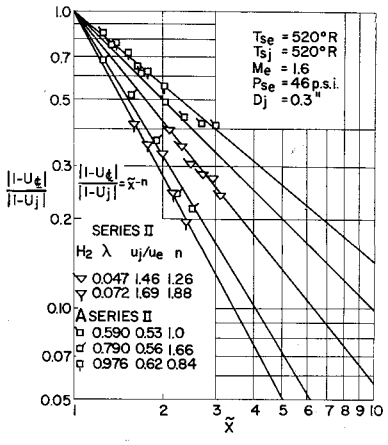

Fig. 6 Velocity decay at the centerline in the mixing region of the jet.

When the mass flux inside the boundary layer is of the same order as that of the injected gas, the initiation of the mixing process is advanced and starts close to the jet discharge, resulting in a decrease of the initial length. This is the case for the data of Ref. 11. There, the mass flux inside the boundary layer was considerably larger than the one in the present test series, and the initial length is about 40% shorter. A similar behavior is noted for the data of Ref. 13: As λ decreases, the influence of the boundary layer becomes more significant and the data deviate from the general trend. Further investigation with respect to the near field of the jet is necessary for a more detailed understanding of the mixing process in this region. Some results pertaining to the near zone were already obtained in Ref. 19.

To investigate the similarity of the radial concentration profiles, Eqs. (25) were applied to the experimental data. The correlation of the normalized profiles in terms of $\bar{r}/\lambda^{k_{Y_2}}\tilde{x}^{m_{Y_2}}$ is shown for H_2 and A in Figs. 4 and 5. It is clearly seen that the profiles exhibit similarity behavior. (For the sake of brevity, only these two profiles have been included. The detailed analysis of the radial profiles for all test series is given in Ref. 22.)

The procedure as outlined previously was also used for the analysis of the velocity profiles in the different flow fields. However, the experimental velocity profiles were not as accurate as the concentration profiles since the determination of the velocity required the measurements of concentration, static, stagnation pressure, and stagnation temperature, resulting in a considerable accumulation of errors in several test series, especially in the H_2 series. Figure 6 presents the centerline velocity decay for H_2 (series II) and for A (series II). The other cases are not reported here since either the initial velocity ratio was close to one, such that no decay could be observed, or the quantity $|1 - U_{\ell}|/|1 - U_i|$ was less than 0.1. The velocity decay along the centerline varied between $\tilde{x}^{-1}$ and $\tilde{x}^{-2}$ and did not exhibit a unique form in contrast to the concentration decay. Another difficulty is encountered in the determination of the length of the potential core for the velocity due to large pressure variations in the near field of the jet.[13]

Figure 7 presents the radial velocity profiles for A (series II) as a function of the correlation parameter $\bar{r}/\lambda^{k_u}\tilde{x}^{m_u}$, and the similarity of the velocity profiles is clearly indicated.

With these profiles, the transport properties can now be determined. Figure 8 presents the diffusion coefficients at the centerline as a function of the mass concentration. The values obtained vary between 0.3 and 0.7 ft²/sec, indicating that the dependence on the concentration is very small. Figure 8 also includes the measurements of Ref. 18. These measurements were obtained in the wake of a two-dimensional porous cylinder. Helium and argon were injected normal to the surface of the cylinder, and the diffusion coefficient was calculated from the concentration and velocity measurements. It is interesting to note that the present measurements differ from those of Ref. 18 only by a factor of 2–6, in spite of the fact that the latter were obtained at a much lower pressure level. This indicates that the turbulent diffusion coefficient does not strongly depend on the pressure level as in the case of laminar flows. It is also concluded from the present experimental data and those of Ref. 18 that turbulent diffusion is almost independent of the molecular weight of the injected gas, since no distinct trend could be observed for H_2, H_e, or A. It is also indicated here that the turbulent diffusion coefficients are about 10^3 times larger than the laminar values which range from 10^{-4} to 7×10^{-3} ft²/sec for the given test conditions.[20]

Figure 9 shows the turbulent viscosity $\rho\epsilon$ at the centerline evaluated from Eqs. (10) and (29). The data vary between 3×10^{-4} and 3×10^{-3} lb-sec/ft², and the scattering is mainly due to the different centerline decay of the velocity obtained in the experiments.

In Sec. 3 it was shown that the eddy viscosity and the turbulent diffusion coefficient were proportional to the product of the half boundary and the centerline velocity. This result was based on the case in which the centerline decay

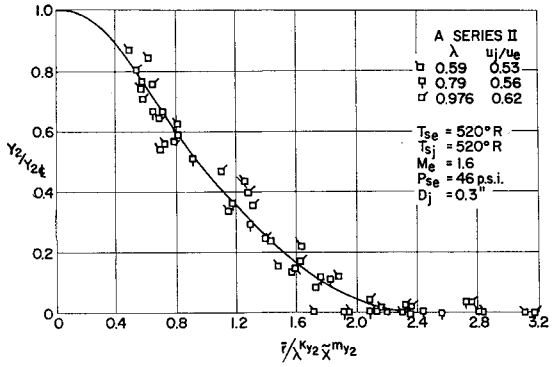

Fig. 5 Correlated radial mass concentration profiles for argon.

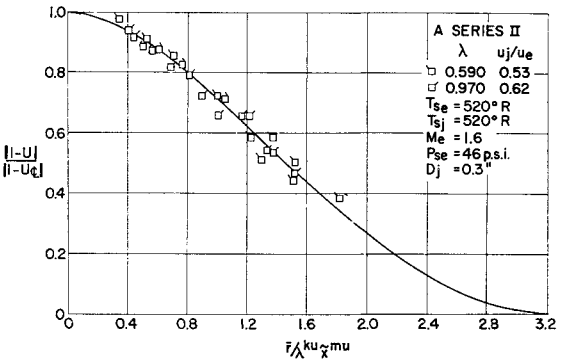

Fig. 7 Correlated radial velocity profiles for argon.

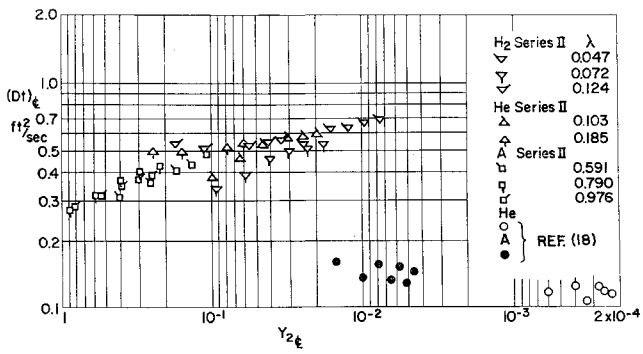

Fig. 8 Turbulent diffusion coefficients as a function of mass concentration at the centerline.

of the velocity parameter $(1 - u_{\ell}/u_e)/(1 - u_j/u_e)$ and the mass concentration $(Y_{2\ell})$ was proportional to $\tilde{x}^{-2}$. To check the validity of these formulations, the solution of Ref. 4 was used to determine the flow properties for the case of H_2, $\lambda = 0.072$, where the experimental decay for both concentration and velocity was equal to $\tilde{x}^{-2}$.¶ The application of the solution of Ref. 4 was justified since the experimentally determined Sc_t number was close to unity. After obtaining the solution in the ψ, ξ plane and specifying the form of the eddy viscosity or turbulent diffusion coefficient, the transformation to the physical plane can then be made through Eqs. (15), and the centerline decay can be determined. This procedure provides a check of the formulations for the eddy viscosity Eq. (33), the turbulent diffusion coefficient Eq. (35), and also a means for comparison with other existing formulations. For this purpose, the following formulations were applied to the solution of Ref. 4:

Prandtl's original formulation, hereafter referred to as formulation (A), is

$$\epsilon = 0.025\, u_e r_0 \bar{r}_{1/2} |1 - U_{\ell}| \qquad \text{(A)}$$

the formulation in Ref. 12 is

$$\rho\epsilon = 0.025\, u_e r_0 \bar{r}_{1/2} |\rho_e - \rho_{\ell} U_{\ell}| \qquad \text{(B)}$$

the one given in Eq. (33) of the present analysis is

$$\epsilon = 0.011\, u_e r_0 \bar{r}_{1/2} U_{\ell} \qquad \text{(C)}$$

and the one for the turbulent diffusion coefficient Eq. (35) is

$$D_t = 0.028\, u_e r_0 \bar{r}_{1/2} U_{\ell} \qquad \text{(D)}$$

The comparison of the results is shown in Fig. 10. It is clearly seen that formulations (A) and (B) give an incorrect

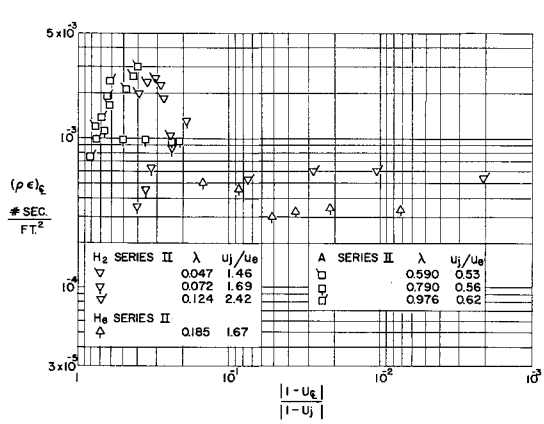

Fig. 9 Turbulent viscosity as a function of the velocity parameter at the centerline.

¶ An equal decay for concentration and velocity implies a constant Sc_t number.

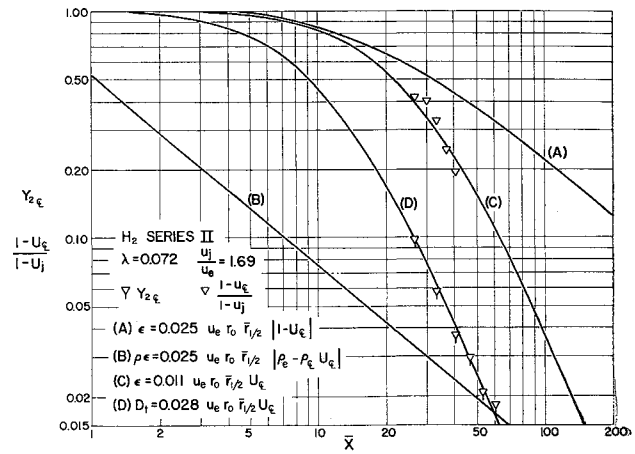

Fig. 10 Comparison of calculated centerline decays with different formulations for the eddy viscosity.

stretching of the axial coordinate, whereas formulations (C) and (D) agree with the experimental data when the constants K_2 in Eq. (33) and K_3 in Eq. (35) are given as in formulations (C) and (D). The predicted centerline concentration decay of $\tilde{x}^{-2}$ obtained by using formulation (C) in the solution of Ref. 4 was also compared to the experimental data of five different test series of H_2[11, 13] where the Sc_t numbers differed from unity. In all cases, formulation (C) agreed with the experimental data when corrected by a multiplicative factor. This indicates that the assumption of a Sc_t number equal to one is valid for the determination of the concentration decay.

Reference 21 applies formulations (A) and (B) in order to determine the flow characteristics in the problem of the turbulent wake. Depending on which formulation was used, the results differed considerably; this discrepancy is also noticed in Fig. 10. Both formulations give a remarkable difference in the form of the decay.

The radial dependence of ϵ and D_t can be investigated through Eq. (6). Using Eq. (26) for the representation of the velocity profile, and assuming constant density [as it was the case for (A)], Eq. (6) can be integrated. The results of the integration proved to be inaccurate since the exponential form of Eq. (26) caused the radial profiles for the eddy viscosity to diverge asymptotically. For this reason, Eq. (26) was replaced by Forstall and Shapiro's cosine profile.[1] This profile gives asymptotically an incorrect description of the velocity decay since the external velocity is reached where $r/r_{1/2} = 2$, but the integral curves of Eq. (6) are well-behaved. The results of a sample calculation for the dependence of the eddy viscosity on the radial coordinate r are shown in Fig. 11 (G series of Ref. 1 with $u_e = 45$ fps and $u_j = 90$ fps). The profiles $\epsilon/\epsilon_{\ell} = f(r/r_{1/2})$ were calculated for six different x stations, $\tilde{x} = 5, 6, 7, 8, 9, 10$. It is seen in Fig. 11 that the profiles are almost the same for all x stations, and ϵ/ϵ_{ℓ} decreases to approximately 0.8 where $r/r_{1/2} = 1$. Between $r/r_{1/2} = 1$ and $r/r_{1/2} = 2$, ϵ/ϵ_{ℓ} decreases eventually to zero.

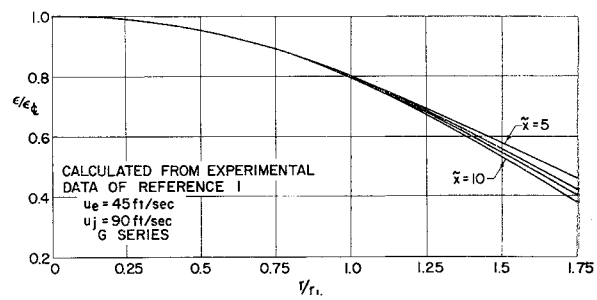

Fig. 11 Radial profiles of the eddy viscosity in low-speed flows.

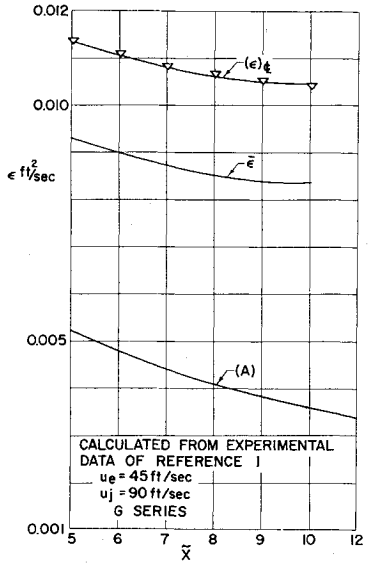

of the eddy viscosity measured in low-speed flows with Prandtl's formulation (A).

In order to compare these results to Prandtl's formulation, the mean values of ϵ/ϵ_{ℓ} for the cross section were evaluated from Fig. 11. Figure 12 presents the centerline values ϵ_{ℓ}, the mean values $\bar{\epsilon}$, and ϵ obtained from Prandtl's formulation. The difference between $\bar{\epsilon}$ and ϵ is about 100%. An adjustment by a constant factor is not possible in this case, since the experimental data approach a constant value as $\bar{x}$ increases, while ϵ obtained from Prandtl's formulation approaches zero. This comparison confirms the results shown in Fig. 10, that the axial coordinate is in error when Prandtl's formulation is used in the transformation equation.

Figure 13 presents the Sc_t numbers along the centerline for three different gases investigated in series II for H_2, series II for He, and series II for A. The values vary from about 0.3 to 2.3 and show no dependence on the molecular weight of the gas. Figure 14 shows the turbulent Lewis number as a function of the mass concentration at the centerline. The data obtained from Eq. (13) vary between 0.4 and 1.0 averaging to a value of about 0.7–0.8. Here again, no dependence on the molecular weight could be observed.

An error analysis was performed for the case of A(λ = 0.590) in Ref. 22. The error for the turbulent D_t, Sc_t, Le_t, and ϵ along the centerline did not exceed $\pm 15\%$ of the mean value obtained for these transport coefficients.

6. Conclusions

The conclusions to be drawn from the present analysis may be stated as follows:

1) The form of the centerline decay of the mass concentration in the mixing region of two coaxial jets is proportional to $\bar{x}^{-2}$ for all test conditions investigated. It is independent of the molecular weight of the injected gas and is affected neither by the variation of the static pressure observed in the near zone of the jet, nor by the boundary layer on the inner jet. Further experimental investigation is required to substantiate whether this $\bar{x}^{-2}$ behavior in the concentration is universal for coaxial compressible (high Mach number and large density gradients) jets.

2) The length of the concentration potential core $\bar{x}_0$ was found to be proportional to the square root of the mass flux ratio $\lambda = \rho_j u_j/\rho_e u_e$. The experiments indicated that the length of the potential core is also influenced by the boundary layer on the inner jet.

3) The radial concentration profiles become similar after a short distance downstream from the potential core and can be correlated by the mass flux parameter λ.

4) No unique centerline decay for the velocity could be observed. The velocity decays obtained in the present experiments vary between x^{-1} and x^{-2}.

5) The radial velocity profiles exhibit similarity behavior and can also be correlated by λ; however, in some cases, this correlation was handicapped by the inaccuracy of the measurement.

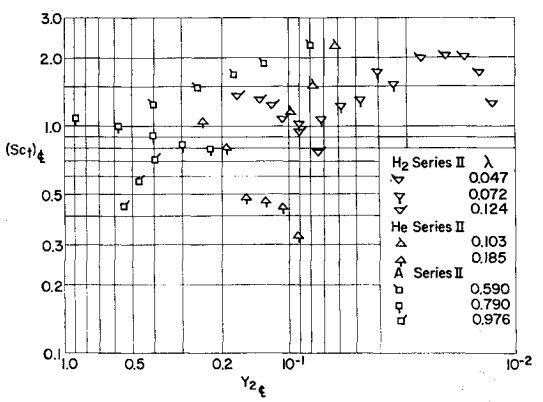

Fig. 13 Turbulent Schmidt number as a function of centerline mass concentration.

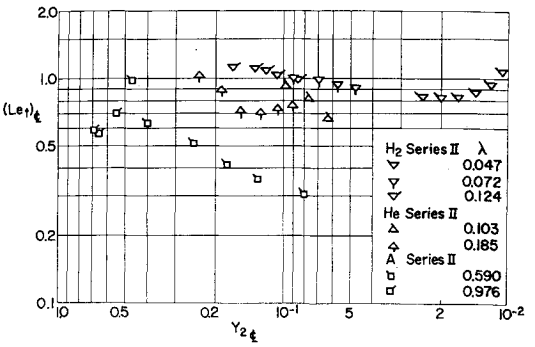

Fig. 14 Turbulent Lewis number as a function of centerline mass concentration.

6) An analysis of the radial variation of the eddy viscosity, using the experimental data of Ref. 1, shows that ϵ decreases to 0.8 of the centerline value at the half boundary $r_{1/2}$.

7) It is concluded from the experimental results that the eddy viscosity as well as the turbulent diffusion coefficient can be expressed as $\epsilon \sim D_t \sim Kr_{1/2}U_{\ell}$, when the form of the decay for both concentration and velocity is the same and equal to $\bar{x}^{-2}$. If the velocity decay differs from $\bar{x}^{-2}$, Eqs. (29) or (31) should be used to evaluate the eddy viscosity ϵ.

8) The analysis of Ref. 4, when extended for arbitrary Schmidt number with the eddy diffusivity developed here, yields the correct concentration decay.

9) Turbulent diffusion coefficients determined from the present experimental data are independent of the molecular weight of the injected gas. They range from 0.3 to 0.6 ft²/sec and are 10^3 times larger than the laminar predictions. The turbulent viscosity $\rho\epsilon$ varied between 3×10^{-4} and 3×10^{-3} lb-sec/ft² for the present test data.

10) The turbulent Schmidt numbers and Lewis numbers determined from the experiments ranged from 0.3 to 2.3 and 0.4 to 1.0, respectively. No dependence on the molecular weight of the injected gas could be observed.

11) The deviation of the turbulent Schmidt number and Lewis number from unity is considerable in several cases. Therefore care must be exercised when solutions, which are based on the assumption of these properties being equal to unity, are used for the determination of the flow characteristics in the mixing region.

12) Additional measurements are necessary in order to clarify the variation of velocity decay in the mixing region.

References

[1] Forstall, W., Jr. and Shapiro, A. H., "Momentum and mass transfer in coaxial jets," J. Appl. Mech. **17**, 399–408 (1950).

[2] Squire, H. B. and Trouncer, J., "Round jets in a general stream," Aeronautical Research Council TR R & M 1974 (1944).

[3] Ferri, A., "Axially symmetric heterogeneous mixing," International Union of Theoretical and Applied Mechanics, International Symposium on Applications of the Theory of Functions in Continuum Mechanics (September 18–24, 1963); also Polytechnic Institute of Brooklyn, PIBAL Rept. 787, Air Force Office of Scientific Research, AFOSR 5326 (September 1963).

[4] Libby, P. A., "A theoretical analysis of the turbulent mixing of reactive gases with application to the supersonic combustion of hydrogen," ARS J. **32**, 388 (1962).

[5] Kleinstein, G., "On the mixing of laminar and turbulent axially symmetric compressible flows," Polytechnic Institute of Brooklyn, PIBAL Rept. 756 (February 1963); also Aeronautical Research Laboratory, ARL 63-108 (June 1963); also "Mixing in turbulent axially symmetric free jets," J. Spacecraft Rockets **1**, 403–408 (1964).

[6] Keagy, W. R. and Weller, A. E., "A study of freely expanding inhomogeneous jets," *Proceedings of the Heat Transfer and Fluid Mechanics Institute* (American Society of Mechanical Engineers, New York, 1949), pp. 89–98.

[7] Maczynski, J. F. J., "A round jet in an ambient coaxial stream," J. Fluid Mech. **13**, 597–608 (1962).

[8] Abramowich, G. N., "Mixing turbulent jets of different density," Izv. Akad. Nauk SSSR, Otd. Tekhn. Nauk, Mekhan. Mashinostr. (1961).

[9] Ragsdale, R. G. and Weinstein, H., "On the hydrodynamics of a coaxial gas flow reactor," ARS/ANS/AS Nuclear Propulsion Conference (August 1962).

[10] Morton, B. R., "Coaxial turbulent jets," J. Heat Mass Transfer **5**, 955–965 (1962).

[11] Alpinieri, L. J., "An experimental investigation of the turbulent mixing of non-homogeneous coaxial jets," Polytechnic Institute of Brooklyn, PIBAL Rept. 789 (August 1963); also "Turbulent mixing of coaxial jets," AIAA J. **2**, 1560–1568 (1964).

[12] Ferri, A., Libby, P. A., and Zakkay, V., "Theoretical and experimental investigation of supersonic combustion," *High Temperatures in Aeronautics* (Pergamon Press, New York, 1962), pp. 55–118.

[13] Zakkay, V. and Krause, E., "Mixing problems with chemical reactions," *Supersonic Flow, Chemical Processes and Radiative Transfer* (Pergamon Press, New York, 1964), pp. 3–29.

[14] Schlichting, H., *Boundary Layer Theory* (McGraw-Hill Book Co., Inc., New York, 1960), 4th ed., Chap. XXIII.

[15] Penner, S. S., *Chemistry Problem in Jet Propulsion* (Pergamon Press, New York, 1951), Chap. XIX.

[16] Hayes, W. D. and Probstein, R. F., *Hypersonic Flow Theory* (Academic Press, New York, 1959), Chap. VIII.

[17] Masters, J. I., "Some applications in physics of the P-function," J. Chem. Phys. **23**, 1865–1874 (1955).

[18] Kingsland, L., Jr., "Experimental study of helium and argon diffusion in the wake of a circular cylinder at $M = 5.8$," Guggenheim Aeronautical Lab., California Institute of Technology, Hypersonic Research Project Memo 60 (June 1, 1961).

[19] Forde, S. M., "An experimental investigation of the mixing of supersonic turbulent streams of non-similar fluids," McGill Univ., Montreal, Rept. 63-3 (April 1963).

[20] Hirschfelder, J. O., Curtiss, C. F., and Bird, R. B., *Molecular Theory of Gases and Liquids* (John Wiley and Sons, Inc., New York, 1954).

[21] Wan, K. S., "Turbulent wake characteristics with different eddy viscosity coefficients," AIAA J. **2**, 121 (1964).

[22] Zakkay, V., Krause, E., and Woo, S. D. L., "Turbulent transport properties for axisymmetric heterogeneous mixing," AIAA Preprint 64-99; also Polytechnic Institute of Brooklyn, PIBAL Rept. 813 (March 1964).